Manuscript Details

Manuscript number	IPVP_2019_102_R1
Title	Thermal and Stress Analyses of a Novel Coated Steam Dual Pipe System for Use in Advanced Ultra-supercritical Power Plant
Article type	Research paper

Abstract

Improving the energy efficiency of advanced ultra-supercritical power plants, by increasing steam operating temperature up to 700°C, can be achieved, at reduced cost, by using novel engineering design concepts, such as coated steam pipe systems manufactured from high temperature materials commonly used in current operational power plants. This paper describes a preliminary feasibility analysis of the design concept of a novel coated dual pipe system under steady-state operation, using analytical and finite element models to evaluate the possible thermal gradients and stresses generated. The results show that the protective coating layer contributes to the effective reduction in the surface temperature of the primary steel pipe. Thermal stresses generated due to the significant difference in the thermal and mechanical properties of the coating and substrate pipe are larger than the mechanical stresses generated by the combined effects of the internal steam pressure in the primary steam pipe and external pressure from the counter-flow cooling steam during steady-state operation. Compared with the stress relaxation of the coating and substrate pipe, creep has a significant impact on the stress distribution within the coating layer. Several key factors have been identified, such as the coating thickness, conductivity, thermal expansion, heat transfer coefficient of cooling steam, cooling steam temperature and cooling steam pressure, which are found to govern thermal and stress distributions during steady-state operation.

Keywords	Advanced ultra-supercritical, Thermal barrier coating, Dual pipe system, Thermal and stress analyses, Creep

Corresponding Author	xiaofeng guo
Order of Authors	xiaofeng guo, Wei Sun, Adib Becker, Andy Morris, Martyn Pavier, Peter Flewitt, Michael Tierney, Christopher Wales

Suggested reviewers	Wenchun Jiang, Haofeng Chen, John Francis, Jianming Gong, Adil Benaarbia

Submission Files Included in this PDF

File Name [File Type]

Cover letter.docx [Cover Letter]

Detailed Responses to the reviewer comments.docx [Response to Reviewers]

Highlights.docx [Highlights]

Manuscript-revised.docx [Manuscript File]

Figures-revised.docx [Figure]

Tables-revised.docx [Table]

To view all the submission files, including those not included in the PDF, click on the manuscript title on your EVISE Homepage, then click 'Download zip file'.

Research Data Related to this Submission

There are no linked research data sets for this submission. The following reason is given:
The data that has been used is confidential

Dr. Xiaofeng Guo
Department of Mechanical, Materials and Manufacturing Engineering
University of Nottingham
University Park
Nottingham NG7 2RD
United Kingdom
xiaofengzidane@gmail.com
March 20, 2019

Dear Editor,

We would like to submit the enclosed manuscript entitled "Thermal and Stress Analyses of a Novel Coated Steam Dual Pipe System for Use in Advanced Ultra-supercritical Power Plant ", which we wish to be considered for publication in **International Journal of Pressure Vessels and Piping** .

Improving the energy efficiency of advanced ultra-supercritical power plants, by increasing steam operating temperature up to 700℃ , can be achieved, at reduced cost, by using novel engineering design concepts, such as coated steam pipe systems manufactured from high temperature materials commonly used in current operational power plants. This paper presents a novel design of a coated steam dual pipe system. An analytical model is then developed to analyze the temperature profiles and thermal stress distributions within the system during steady state operation. Additionally, thermal and stress analyses together with creep relaxation analysis of the dual pipe system during steady state operation are performed using the finite element analysis. Finally, the effects of several key factors such as the TC thickness, TC conductivity, thermal expansion coefficient of the TC, cooling steam temperature and pressure, on the thermal and stress distributions are also discussed.

Meanwhile, I have read and have abided by the statement of ethical standards for manuscripts submitted to **International Journal of Pressure Vessels and Piping**. This work described has not been submitted elsewhere for publication, in whole or in part, and all the authors listed have approved the manuscript that is enclosed.

The corresponding author is Dr. Xiaofeng Guo, and the E-*mail address:* xiaofengzidane@gmail.com. Other information is as follows:

Address: Department of Mechanical, Materials and Manufacturing Engineering, University of Nottingham, Nottingham NG7 2RD, United Kingdom.
Tel.: 0115 951 3809
Fax: 0115 951 3800

Thank you very much for your attention and consideration to our paper.

Best wishes.

Sincerely Yours,
Xiaofeng Guo

Dear editor and reviewers,

Thank you for your useful comments and suggestions. We have answered your questions, and modified the manuscript accordingly. The detailed corrections are listed below point by point:

-Reviewer 1

1. After Eq2, "and ki are" must be replaced by "and ki(r) are". Please add a white space between the math symbols and the text in the whole manuscript.
   - ✓ Thank you for your useful suggestions. In the revised version, I have replaced k_i by $k_i(r)$, and add a white space between the math symbols and the text in the whole paper.

2. Please use a unique notation for the logarithmic symbol in Eqs 4, 6 and 7.
   - ✓ Yes, I have made the changes in the revised manuscript.

3. In page 5, equations of the boundary conditions used to identify the Ai and Bi constants should be written in the text?
   - ✓ According to your suggestions, I have added the equations (equations (4) and (5)) of the boundary conditions to identify A_i and B_i. Please see the details in the updated paper.

4. The material parameters used for the elastoplastic models should be cited somewhere in the paper. The yield strength values for the P91 steel are overestimated (see Table 2). A classical anisothermal and unified viscoplastic model (Chaboche-type) can also be used to investigate the pipe system!!
   - ✓ In this study, the material parameters used for the elasto-plastic models are taken from the available literature. Some references have been cited in the paper. At present, P91 steel can be produced by many manufacturers in the world. The yield strength values for the P91 steel vary from the cast to cast, although the specification, ASME SA-335-2007 [1], sets minimum requirements for material strength. In this study, the yield strength values for the P91 steel were obtained from Vallourec & Mannesmann (V&M) Tubes Corp., as shown in Fig.1 [2]. It is well known that V&M is the world leader in offering a premium range of tubes including seamless tubes and line pipes. Therefore, we believe the yield strength values for the P91 steel from V&M are reasonable and reliable.

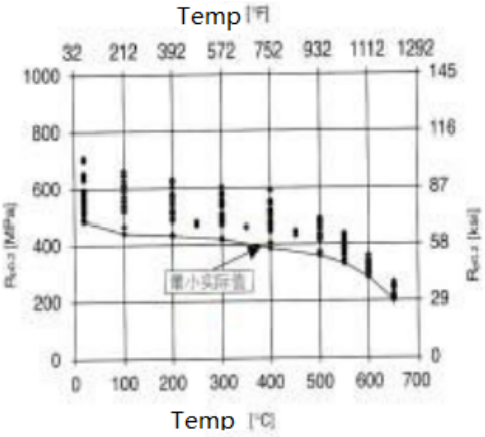

Fig. 1 Variation of the yield strength of P91 steel with temperature [2]

In this paper, we just tried to build a system analysis model and considered the effect of some key factors on the temperature and stress distributions for a concept proof study. Definitely, the effect of cycling is very important, and a classical anisothermal and unified viscoplastic model can be used to study the dual pipe system [3]. Relevant research work is still in progress, and we will report it in the future paper.

5. An interesting result is observed for both interfaces TC/BC and BC/P91 (see Fig 6). The discontinuity of stresses needs to be explained with regards to the high values reported for the hoop stress in Fig 4 (the hoop stress magnitudes are significantly higher than the applied stresses 35MPa and 7.5MPa).

✓ In this study, the results shown in Fig.6 can be obtained by using the following boundary conditions

$$\sigma_{r_i}(R_1) = -P_i \tag{1}$$

$$\sigma_{r_n}(R_n) = -P_o \tag{2}$$

where $\sigma_{r_i}(R_1)$ and $\sigma_{r_n}(R_n)$ are axial stresses on the inner and outer walls, P_i and P_o are the internal and external pressures.

Additionally, the interface displacement continuous conditions are also used

$$u_i(R_i) = u_{i+1}(R_i), \quad i=1,\ 2,\ \cdots,\ n\text{-}1 \tag{3}$$

where $u_i(R_i)$ denotes the radial displacement at the i-th layer. These boundary conditions and interface displacement continuous conditions result in the continuous distribution of radial stress in the dual pipe system, whereas hoop stress is discontinuous across the interfaces.

In this dual pipe system, the total stress includes thermal stress and mechanical stress. For the mechanical stress, the internal and external pressures are 35 MPa and 7.5 MPa, respectively. These mechanical loadings can result in the axial stress, hoop stress and radial stress in the system. In the current axisymmetric model, the possible hoop stress generated is significantly high than the radial stress, as shown in Fig.6 (b). On the other hand, the possible thermal stress generated by a thermal gradient also includes the axial stress, hoop stress and radial stress in the system. Also, hoop stress generated by the thermal loading is significantly high than the radial stress. Compared with Fig.6 (a) and Fig.6 (b), it can be seen that thermal stress magnitudes generated by thermal gradients are much higher than the mechanical stress values. Therefore, the hoop stress magnitudes generated by the thermal and mechanical loadings are significantly higher than the internal and external pressures (35 MPa and 7.5 MPa).

-Reviewer 2

1. In the 2ed paragraph of Page 3, what do you mean by "therefore stress distribution of the system"?
   - ✓ It is well known that the use of TBCs, along with internal cooling of the underlying steel component, provide major reductions in the surface temperature of the substrate. Therefore, there is a significant temperature gradient between the coating and the substrate. Due to the great difference in the thermo-mechanical properties of ceramics (the coating) and metals (the substrate), thermal-expansion mismatch stress between the coating and the substrate will be enhanced in the TBCs system. Generally, this mismatch stress can affect the total stress distribution of the system.

2. In the 2ed paragraph of Page 3, "The combination of these effects will therefore govern the temperature and stress distributions of the system during service conditions.", 'TBC' should be added before 'system'.
   - ✓ Yes, I have modified it.

3. In the 2ed paragraph of Page 3, "Owing to the high oxidation resistance of MCrAlY alloys, NiCoCrAlY is chosen as the candidate BC in this study.", the author emphasizes that NiCoCrAlY is chosen as the BC in the current study due to its high oxidation resistance, however, the BC may not be suffered from oxidation because it located between the TC and the substrate P91 steel, please explain.
   - ✓ Generally, the bond coat (BC) is an oxidation metallic layer, 50-150 μ m in thickness. At peak operating conditions, the bond-coat temperature in the coated dual pipe system typically exceeds 580℃ , resulting in bond-coat oxidation and the inevitable formation of a third layer -- the thermally grown oxide. The interconnected porosity that always exists in the top-coat allows easy ingress of oxygen from the high-temperature steam environment to the

bond coat. Moreover, even if the top-coat were fully dense, the extremely high ionic diffusivity of oxygen in the ZrO_2-based ceramic top-coat renders it "oxygen transparent" [4]. Therefore, NiCoCrAlY is chosen as the candidate BC in this study, owing to its high oxidation resistance.

4. In Fig.4, please add the boundaries of TC, BC and P91 in the contour plot so that it is easily found where is the interface between different materials.

✓ In this dual pipe system, the total thickness of the TC, BC and P91 is 63 mm, while the thickness of the BC is only 0.5 mm. Due to the limitation of geometric dimension, we cannot see the interfaces clearly, even if the boundaries of TC, BC and P91 in the contour plot is added in Fig.4. Thus, we neglect the boundaries of TC, BC and P91 in Fig.4, and its characteristics of the interfaces are illustrated in Fig.5 instead.

5. In Fig. 7, it is better to show the stress variation behavior across the whole system instead of only BC.

✓ Thank you for your suggestion. As described in the manuscript, compared with the creep stress relaxation behavior during the long-term creep exposure, creep does not have a significant influence on the stress distribution of the TC and substrate. So it is important to show the stress relaxation behavior of the BC. Moreover, the total thickness of the dual pipe system (TC, BC and substrate) is 63 mm, while the thickness of the BC is 0.5 mm. We tried to exhibit the stress variation behavior across the whole system, but it is difficult to show the good picture quality due to the small thickness of the BC. Actually, in this paper we think it is enough to show the stress relaxation of the BC layer before and after creep exposure.

6. In sub-section 4.3, the author mainly describe the stress relaxation behavior, why the creep strain which is the key factor indicating failure was not discussed?

✓ This paper describes a preliminary feasibility analysis of the design concept of a novel coated dual pipe system under steady-state operation. The key topic of this paper is to evaluate the possible thermal gradients and stresses generated, but not the strains. Although creep stain is a key factor indicating failure, we don't want to discuss the creep stain in this paper because of the space limitation.

7. Which method was used to get the results of Figs. 9-12, analytical solution or FEM? Please indicate.

✓ In this investigation, thermal and stress analyses are performed using the finite element analysis. Here, we get the results in Figs. 9-12 using FEM.

8. In the legend of Fig.11 "top coating" should be replaced by "TC".

✓ Yes, I have replaced "TC" with "top coating".

9. In the point 5 of conclusion part, the author are suggested to indicate the most sensitive factor among these investigated parameters.

- ✓ As reported in the conclusion, several key governing parameters, such as the coating thickness, conductivity, thermal expansion, heat transfer coefficient of cooling steam, cooling steam temperature and cooling steam pressure, are found to have a significant effect on thermal and stress distributions during steady-state operation. Compared with other material properties and operating parameters, the coating thickness may be the most sensitive factors among the parameters. According to the comments from the reviewer, we have refined sensitive factors, and listed in the conclusion.

References

[1] ASME SA-335, Specification for seamless ferritic alloy- steel pipe for high-temperature service [S]. 2007.

[2] Vallourec & Mannesmann Tubes. T/P91 tubing handbook[R]. Boulogne France: Vallourec & Mannesmann Tubes, 2012 (in Chinese) https://wenku.baidu.com/view/7c66d4282af90242a895e56b.html

[3] A. Benaarbia, J.P. Rouse, W. Sun, A thermodynamically-based viscoelastic-viscoplastic model for the high temperature cyclic behaviour of 9–12% Cr steels, International Journal of Plasticity 107 (2018) 100–121.

[4] N.P. Padture, M. Gell, E.H. Jordan, Thermal barrier coatings for gas-turbine engine applications, Science 296 (2002) 280-284.

Highlights:

► An analytical model is developed which is capable to calculate the temperature profiles and thermal stress fields of the coated steam dual pipe system.

► Thermal stresses generated due to the thermal gradient through the pipe wall are larger than the mechanical stresses.

► Creep has a significant impact on the stress distribution within the coating layer.

► Several key governing parameters are found to have a significant effect on thermal and stress distributions.

Thermal and Stress Analyses of a Novel Coated Steam Dual Pipe System for Use in Advanced Ultra-supercritical Power Plant

Xiaofeng Guo [a,*], Wei Sun [a], Adib Becker [a], Andy Morris [b], Martyn Pavier [c], Peter Flewitt [c], Michael Tierney [c], Christopher Wales [c]

[a] Department of Mechanical, Materials and Manufacturing Engineering, University of Nottingham, Nottingham, NG7 2RD, UK

[b] EDF Energy (UK), Coal Gas and Renewables, Central Technical Organisation, Barnwood, Gloucester, GL4 3RS, UK

[c] Department of Mechanical Engineering, University of Bristol, Bristol, BS8 1TR, UK

Abstract: Improving the energy efficiency of advanced ultra-supercritical power plants, by increasing steam operating temperature up to 700℃, can be achieved, at reduced cost, by using novel engineering design concepts, such as coated steam pipe systems manufactured from high temperature materials commonly used in current operational power plants. This paper describes a preliminary feasibility analysis of the design concept of a novel coated dual pipe system under steady-state operation, using analytical and finite element models to evaluate the possible thermal gradients and stresses generated. The results show that the protective coating layer contributes to the effective reduction in the surface temperature of the primary steel pipe. Thermal stresses generated due to the significant difference in the thermal and mechanical properties of the coating and substrate pipe are larger than the mechanical stresses generated by the combined effects of the internal steam pressure in the primary steam pipe and external pressure from the counter-flow cooling steam during steady-state operation. Compared with the stress relaxation of the coating and substrate pipe, creep has a significant impact on the stress distribution within the coating layer. Several key factors have been identified, such as the coating thickness, conductivity, thermal expansion, heat transfer coefficient of cooling steam, cooling steam temperature and cooling steam pressure, which are found to govern thermal and stress distributions during steady-state operation.

Keywords: Advanced ultra-supercritical, Thermal barrier coating, Dual pipe system, Thermal and stress analyses, Creep

*Corresponding author.

E-*mail address:* xiaofengzidane@gmail.com (Xiaofeng Guo)

1. Introduction

In the 21st century, worldwide energy shortage and growing global pollution drive the development of ultra-supercritical technology. Recently, several advanced ultra-supercritical power plants with target steam temperature up to 700℃ are proposed to further improve the thermal efficiency of power plants and reduce fuel consumption and CO_2 emissions [1-3]. Using conventional steam cycle design, such high operation temperature will require the use of nickel-based alloys, such as Inconel 740, Haynes 230 and CCA 617, for the components in superheaters, reheaters and steam transfer pipes, owing to their better resistance to creep damage and steam oxidation[4-5]. However, high cost and scarce supply of these alloys hinder the development of today's state-of-the-art advanced ultra-supercritical technology. An alternative plant design is therefore required to achieve higher steam operating temperatures at an acceptable cost.

In the past decades, thermal barrier coatings (TBCs), especially partially stabilized zirconia-yttria (YSZ), have been widely used in aircraft and industrial gas-turbine engines to provide thermal insulation and oxidation protection for the superalloy structures [6-8]. Based on this system design philosophy, an innovative steam transfer piping system, operating at temperature up to 700℃, without the use of nickel-based alloys could be designed using TBCs made of low-thermal conductivity ceramics to reduce the surface temperature of the primary steel pipe. However, due to the different physical, thermal and mechanical properties of ceramics and steels, thermal gradient and thermal-expansion mismatch stress will be generated during operation condition, which greatly influences the structural integrity of the system [9-10]. In order to investigate the feasibility of the coated pipe system, temperature and stress analysis models need to be established for the evaluation of the thermal and stress distributions of the system during steady-state operation. In this design the thermal barrier coating is assumed to comprise a top coat (TC), exposed to high temperature steam conditions at the boiler outlet and a bond coat (BC), which ensures a suitable interface and transition to the primary pipe steel.

Additionally, when the TBC system is operated under the service conditions, stress relaxation of the TC, BC and primary pipe may occur at high temperature [11-14].

Experimentally, creep properties obtained on monolithic specimens and composite coated samples indicate that the creep strain rate of the coating $\dot{\varepsilon}_c$ is strongly dependent on the stress exponent n and the activation energy for creep deformation Q, and the temperature dependent creep relaxation behaviour of the coating material can be expressed by the phenomenological equation [15-17]:

$$\dot{\varepsilon}_c = A\sigma^n exp(-\frac{Q}{RT}) \quad (1)$$

where A is a constant, σ is the applied stress, R is the gas constant, and T is the absolute temperature. In terms of this classical steady-state creep model, a few investigations have been undertaken to study the creep relaxation during service conditions using the finite element method [18-20]. Miller et al [21] have reported that creep resistance of the BC can have a significant effect on the TBC life during thermal cycling, as the stress relaxation of the BC may cause an increase of the stress in the TC layer.

In general, the geometry and material properties of the TBC system, especially those of the TC layer greatly affect the thermal insulation capacity and thermal-expansion mismatch stress distribution of the system. Recent investigations have shown that the effect of thermal insulation of the TC layer increases with the increase of the coating thickness and the decrease of the coating conductivity [22-24]. Simultaneously, thermal-expansion mismatch stress between the TBC and primary steel pipe may be enhanced in the system due to the significant difference in the thermal and mechanical properties of the coating and substrate pipe. Other factors including the operating temperature and pressure can also contribute to the variation in the temperature and stress fields of the TBC system. The combination of these effects will therefore govern the temperature and stress distributions of the TBC system during service conditions. Thus, a detailed parametric analysis of the novel system must be carried out to enable the feasibility of the concept to be properly addressed, owing to the complexity of the key governing variables.

This paper describes a feasibility study associated with the collaborative research program "Novel high temperature steam transfer pipes" [25] with the aim of increasing the operating steam temperature up to 700℃ (and possibly beyond) and steam pressure to about 35 MPa without the need for nickel-based alloys. In the present investigation, a novel design of a coated steam dual pipe system is first introduced. An

analytical model is then developed to analyze the temperature profiles and thermal stress distributions within the system during steady state operation. Additionally, thermal and stress analyses together with creep relaxation analysis of the dual pipe system during steady state operation are performed using the finite element analysis. Finally, the effects of several key factors such as the TC thickness, TC conductivity, thermal expansion coefficient of the TC, cooling steam temperature and pressure, on the thermal and stress distributions are also discussed. For the purposes of this feasibility study only steady-state steam conditions are analysed.

2. The Concept of a Novel Coated Steam Dual Pipe System

2.1 The design principle

In the present study, the design concept entails a novel coated steam dual pipe system, which uses ceramic barrier coating with low-thermal conductivity to provide thermal insulation and oxidation protection to the internal main steam steel pipe, and uses external counter-cooling to limit the operating temperature of the pipe materials, hence avoiding the requirement for the extensive use of advanced nickel-based alloys for the primary steam piping. In terms of this design principle, a novel thermal barrier coated dual pipe system is designed, as shown in Fig. 1.

2.2 System configuration

As shown in Fig. 1, a novel steel pipe system with a ceramic TBC on its internal surface and counter-cooling on its outer surface provided by exhaust steam from the high pressure turbine is proposed [25]. The system comprises a stable TC ceramic layer, a metallic BC layer, internal steam pipe and external cooling steam pipe, as shown in Fig.2. 9-12%Cr creep-strength enhanced ferritic steels are commonly used for high-temperature thick section components in power plants. In the current work, ASME grade P91 steel is selected as the substrate material of the primary steam pipe.

In order to provide the necessary thermal insulation and oxidation protection for the primary steam pipe, YSZ is assumed to be used as the TC. Considering significantly different physical, thermal and mechanical properties of ceramics and steels, the metallic BC layer having intermediate physical properties between the ceramic layer and the steel is designed to generate a compatible oxide to enable the ceramic to adhere to the underlying steel pipe. At peak operating conditions, the interconnected porosity

that always exists in the TC allows easy ingress of oxygen from the high-temperature steam environment to the BC [6]. Owing to the high oxidation resistance of MCrAlY alloys, NiCoCrAlY is chosen as the candidate BC in this study. Additionally, ASME SA213 T23 steel is used as the material of the external (secondary) cooling steam pipe. The key geometries of the coated dual pipe system and the assumed steady-state steam conditions are listed in Table1.

3. Thermal and Stress Models of the Coated Dual Pipe System

3.1 Analytical models of the dual pipe system

3.1.1 System model

In order to investigate the thermal gradient of the coating-pipe system generated during steady-state operation, a one dimensional model of the heat transfer is built up in this study, as shown in Fig. 3. In this model, there are 3 layers, the TC, BC and the substrate pipe. The thicknesses of 3 layers are determined by the thermodynamic modelling of the coated dual pipe system (see. Pavier [25]). Each layer of material has a different conductivity coefficient which can be expressed by k_1, k_2, k_3, respectively. h_t and h_s are the heat transfer coefficients of hot steam and cooling steam, respectively. Here, T_h and T_c define the hot steam temperature and cooling steam temperature. T_1, T_2, T_3 and T_4 stand for the different boundary temperatures of each layer.

3.1.2 Heat transfer analysis

Assuming that the cylinder is infinitely long, a one dimensional equation of heat transfer can be expressed as:

$$\frac{\mathrm{d}}{dr}\left[-rk_i(r)\frac{dT_i(r)}{dr}\right]=0 \tag{2}$$

where T_i(r) and k_i(r) are the temperature and conductivity coefficients at the i-th layer.

In the current work, we assume that the material is homogeneous in each layer. The temperature distribution of the coating-pipe system can be written as:

$$T_i(\mathrm{r}) = -\int_{R_i}^{r}\frac{A_i}{rk_i(r)}dr + B_i \quad (R_1 \le r \le R_{i+1}, i=1,2,3) \tag{3}$$

where A_i and B_i are the integral constants.

The following boundary conditions are used

$$k_1 \frac{dT_1(r)}{dr}\Big|_{r=R_1} = h_t[T_h - T_1(R_1)] \tag{4}$$

$$k_3 \frac{dT_3(r)}{dr}\Big|_{r=R_4} = h_s[T_3(R_4) - T_c] \tag{5}$$

Based on the interface temperature continuous condition and interface heat flow continuous condition, A_i and B_i in equation (3) can be given as:

$$A_i = \frac{T_h - T_c}{\frac{1}{h_t R_1} + \frac{1}{k_1}\ln\left(\frac{R_2}{R_1}\right) + \frac{1}{k_2}\ln\left(\frac{R_3}{R_2}\right) + \frac{1}{k_3}\ln\left(\frac{R_4}{R_3}\right) + \frac{1}{h_s R_4}}, \quad i = 1,2,3 \tag{6}$$

$$B_1 = T_h - \frac{A_1}{h_t R_1} \tag{7}$$

$$B_2 = B_1 - \frac{A_1}{k_1}\ln\frac{R_2}{R_1} \tag{8}$$

$$B_3 = B_2 - \frac{A_2}{k_2}\ln\frac{R_3}{R_2} \tag{9}$$

3.1.3 Thermal stress analysis

Based on the heat transfer model, a thermal stress analytical model of the coating-pipe system is developed in this investigation. In this model, axial stress $\sigma_{r_i}(r)$ and hoop stress $\sigma_{\theta_i}(r)$ at the i-th layer satisfy the following equilibrium equation neglecting the body forces:

$$\frac{d\sigma_{r_i}(r)}{dr_i} + \frac{\sigma_{r_i}(r) - \sigma_{\theta_i}(r)}{r_i} = 0 \tag{10}$$

The following strain- displacement relations and compatibility conditions are adopted

$$\varepsilon_{r_i}(\mathrm{r}) = \frac{du_i(r)}{dr_i} \tag{11}$$

$$\varepsilon_{\theta_i}(\mathrm{r}) = \frac{u_i(r)}{r_i} \tag{12}$$

where $u_i(r)$ denotes the radial displacement, ε_{r_i} and ε_{θ_i} are the radial and hoop strains at the i-th layer.

The radial and hoop stresses can be given as:

$$\sigma_{r_i}(r) = \frac{E_i(1-\nu_i)}{(1+\nu_i)(1-2\nu_i)}[\varepsilon_{r_i}(r) + \frac{\nu_i}{1-\nu_i}\varepsilon_{\theta_i}(r) - \frac{1+\nu_i}{1-\nu_i}\alpha_i \Delta T_i(r)] \quad (13)$$

$$\sigma_{\theta_i}(r) = \frac{E_i(1-\nu_i)}{(1+\nu_i)(1-2\nu_i)}[\varepsilon_{\theta_i}(r) + \frac{\nu_i}{1-\nu_i}\varepsilon_{r_i}(r) - \frac{1+\nu_i}{1-\nu_i}\alpha_i \Delta T_i(r)] \quad (14)$$

where E_i is the modulus of elasticity, ν_i is Poisson's ratio, α_i is the coefficient of linear thermal expansion, $\Delta T_i(r)$ is the change in the temperature at the *i*-th layer.

Substituting equations (13) and (14) into equation (10), $u_i(r)$ can be written as follows:

$$u_i(\mathrm{r}) = \frac{1+\nu_i\alpha_i}{1-\nu_i\, r}\int_{R_1}^{r} \Delta T_i(r) r dr + C_i r + \frac{D_i}{r} \quad (15)$$

where C_i *and* D_i are the integral constants.

Substituting equation (15) into equations (11) and (12), $\sigma_{r_i}(\mathrm{r})$ and $\sigma_{\theta_i}(\mathrm{r})$ at the *i*-th layer can be expressed as:

$$\sigma_{r_i}(r) = -\frac{E_i\alpha_i}{1-\nu_i}\frac{1}{r^2}\int_{R_1}^{r} \Delta T_i(r) r dr + \frac{E_i C_i}{(1+\nu_i)(1-2\nu_i)} - \frac{E_i D_i}{(1+\nu_i)r^2} \quad (16)$$

$$\sigma_{\theta_i}(r) = \frac{E_i}{1-\nu_i}\frac{\alpha_i}{r^2}\int_{R_1}^{r} \Delta T_i(r) r dr + \frac{E_i C_i}{(1+\nu_i)(1-2\nu_i)} + \frac{E_i D_i}{(1+\nu_i)r^2} - \frac{E_i\alpha_i}{1-\nu_i}T_i(r) \quad (17)$$

In the equations (16) and (17), when the index i =1, it is reduced to the stress distribution for linear elastic behaviour of a thick-wall cylinder subjected to a steady-state temperature distribution [26]. In this condition, the accuracy of the theoretical model can be verified against the classical example. When the index i =3, the equations (3), (16) and (17) are used to calculate the thermal and stress distributions of the coated dual pipe system. Also, the analytical solutions are compared with the finite element calculations to assess the accuracy of the analytical solutions.

3.2 Finite element (FE) model of the dual pipe system

In this study, a sequentially coupled thermal-mechanical simulation procedure is developed for the coated dual pipe system. In this method, the uncoupled thermal analysis is first performed in a heat transfer procedure. Then the stress distribution which depends on the temperature distribution is calculated.

3.2.1 Geometry and meshing

A 2-D axisymmetric finite element (FE) model of the coated steam dual pipe system is used in the current study. The inner radius of the TC is 117 mm. The thicknesses of the TC and BC are 2.5 and 0.5 mm, respectively. The inner radius of the primary steam pipe is 120 mm with a wall thickness of 60 mm. The element type used in the temperature and the stress analyses are 8-node isoparametric quadratic axisymmetric temperature and continuum elements with reduced 2× 2 integration (DCAX8 and CAX8R in ABAQUS, respectively). The mesh includes 63,500 elements with 191,755 nodes. The mesh size is fine enough to eliminate its influence, so it guarantees the adequate computational accuracy of the simulations.

3.2.2 Material properties

In this study, it is assumed that the materials of the TC, BC and substrate are isotropic and homogeneous. The elasto-plastic behaviours of the TBC system are considered [27]. Some temperature dependent material properties of the TC, BC and the internal steam pipe required for the FE models, i.e. coefficient of thermal expansion (CTE), conductivity, density and specific heat, can be taken from the available literature [28-31]. Other properties over a wide range of temperatures can be estimated based on linear interpolation of the existing data. These are given in Table 2.

Additionally, since the coated dual pipe system will be subjected to high temperature in actual service conditions, creep analysis of the TBC system is also performed in this investigation. In this work, for simplicity, the effect of creep is described by the Norton power-law creep equation [11, 12, 32-34]:

$$\dot{\varepsilon}_c = B\sigma^n \tag{18}$$

where σ is the applied stress. In this work, the parameters B and n are both temperature dependent, as listed in Table 3.

3.2.3 Boundary conditions

In the coated steam dual pipe system, baseline simulation conditions are set as follows. In order to improve power plant efficiency, the primary steam pipe is assumed to operate with a steam temperature up to 700℃. Meanwhile, cooling

steam at a temperature of 450℃ in the secondary counter-cooled pipe is used to reduce the temperature of the primary steam pipe. Under these operating conditions, the inner surface of the TC is heated from 20℃ to 700℃ by the steam exiting from the combustion boiler, and the external surface of primary steam pipe is heated from 20℃ to 450℃. To reach steady-state conditions, sufficient heating time is set up in the simulation.

Symmetric boundary conditions are applied to the bottom surface of the dual pipe system in the Y-direction, as shown in Fig. 4. The distributed work internal pressure (35 MPa) is imposed on the inner surface of the TC to simulate steady-state steam pressure conditions, and the distributed work external pressure (7.5 MPa) is applied to the outer surface of primary steam pipe.

4. Thermal and Stress Analyses of the Dual Pipe System

4.1 Thermal analysis during steady-state operation

As shown in Fig. 1, in the proposed steam circuit operating under steady-state conditions with well lagged piping, the cooling pipe will be operated at a constant and relatively uniform through-thickness temperature equal to the cooling steam temperature. Little heat transfer will occur from the cooling steam to the cooling pipe. However, for the coated primary steam pipe, the situation will be completely different. Heat will be transferred from the high-temperature steam (at 700℃ and 35 MPa) flowing through the bore of the internal pipe through the coating and then to the primary pipe. On the external surface of the primary steam pipe, heat will be transferred to the cooling steam (at 450℃ and 7.5 MPa). Based on such heat transfer characteristics, thermal analysis of the coated steam pipe system is investigated.

Fig. 4(a) shows the temperature distribution contour plot of the coated primary steam pipe during steady-state operation. It can be seen from Fig. 4(a) that the temperature in the system decreases monotonically through the wall thickness. Compared with the conventional steam cycle system operated at a relative uniform temperature field, the temperature distribution through the wall thickness is uneven in the coated dual pipe system. In the current steam cycle design, owing to the external counter-cooling steam, the temperature gradually decreases through the wall thickness of the primary steam pipe.

Fig. 5 presents the temperature distribution of the coated primary steam pipe through the wall thickness obtained by FE analysis and an analytical solution. It can be seen from this figure that the results obtained from FE are almost identical to the analytical solutions. Due to the lower thermal conductivity of the TBC system, as expected, there is a large temperature gradient between the inner and outer walls of the TBC, which greatly reduces the inner surface temperature of the substrate pipe. In the present model, when the inner surface of the TC is subjected to around 700℃ and the external surface of the primary steam pipe is operated at 450℃, the inner surface temperature of the substrate pipe is about 560℃ under steady-state operation. It clearly indicates that this TBC system can successfully provide sufficient thermal insulation for the primary steam pipe.

4.2 Stress analysis during steady-state operation

Stress distribution contour plots of the coat-primary steam pipe during steady-state operation are shown in Figs. 4(b) and (c). As shown in Fig. 4(b), the radial stress of the system is always compressive, and the negative peak stress value is -41MPa located in the primary steam pipe. It can be clearly seen from Fig. 4(c) that the positive peak value of the hoop stress located on the external surface of the primary steam pipe is 209 MPa. Since the value of the hoop stress is much larger than that of the radial stress, hoop stress plays a significant role in determining the structural integrity of the system. Additionally, the hoop stress gradient at the TC/BC interface is also observed in this study.

In order to understand the stress gradient generated during steady-state operation, the stress distributions, including thermal and mechanical stresses, of the coating-primary steam pipe system along the wall thickness are exhibited in Fig. 6(b), where only the thermal stress distribution of the system is shown in Fig. 6(a) as a comparison. For the coating-primary steam pipe system, it can be seen that compared with the mechanical stress generated by the internal pressure and external pressure, thermal stress produced by the thermal gradient along the wall thickness direction is much larger during steady-state operation. Thus, thermal stress plays a significant role in determining the structural integrity of the coated dual pipe system. Additionally, based on the boundary conditions and interface displacement continuous conditions using in the FE models, radial stress is continuous along the wall thickness direction,

whereas hoop stress is discontinuous across the interfaces. In this investigation, because the total hoop stress in the system is generated by the mechanical and thermal loadings, its magnitudes are significantly higher than the values generated by the internal and external pressures. During the steady-state operation, the radial stress of the system is quite small, and the variation of radial stress along the wall thickness is relatively insignificant.

The variation of hoop stress along the wall thickness is also shown in Fig. 6(b). As mentioned above, in addition to the maximum hoop stress distributed on the external surface of the primary steam pipe, a significant stress gradient is present in the current system due to the thermal-expansion mismatch at the TC/BC interface. The positive hoop stress at the interface is 185 MPa. Because the temperature at the TC/BC interface is about 110℃ higher than the temperature on the outer surface of the primary steam pipe, this interface between the TC and BC may be prone to failure during the high-temperature service conditions.

Meanwhile, the variation of von Mises stress along the wall thickness is shown in Fig. 6(b). The von Mises stress curve has a peak value at the TC/BC interface during the steady-state operation, but the stress is greatly reduced on both sides of the peak. Moreover, it is well-known that some interface geometry factors, such as the roughening at the TC/BC interface during the thermal cycling, the undulated interface as well as the interfacial imperfection, can create out-of-plane stresses normal to the interface [6]. This stress together with the service load may contribute to the formation of cracks and thereby the premature failure of the system. The current results imply that this interface is likely to be the most dangerous region of the failure.

4.3 Stress relaxation

The effect of creep on stress relaxation is taken into account in this work, due to the expected long-term service of the system at elevated temperature. In the current investigation, the key topic of this work is to evaluate the possible stresses generated in the system, not the strains. Thus, only stress analysis results of the TBC system before and after creep are investigated because of the space limitation. The results show that although creep does not have a significant influence on the stress distribution of the TC and substrate, it plays a great role in the stress relaxation of the BC layer. In this dual pipe system, the total thickness of the TC, BC and P91 is 63mm, while the thickness of

the BC is only 0.5 mm. Due to the limitation of geometric dimension, the variation of stress across the BC instead of the whole system before and after 10^5 h creep exposure are exhibited in Fig.7. Note from Fig. 7 that the creep strain of the BC layer greatly reduces the stress level within BC layer induced by the thermal-expansion mismatch. After long-term creep exposure, the maximum tensile stress changes from the TC/BC interface before creep to the BC/substrate interface, and its value reaches 195 MPa. In order to further analyse the stress relaxation behaviour at the TC/BC interface and BC/substrate interface during long-term creep exposure, the stress relaxation profile with creep time is evaluated, as shown in Fig. 8. The results reveal that extensive stress relaxation occurs continuously during the creep exposure. At the TC/BC interface, it can be seen that the stress of 326 MPa is continuously decreased to 179 MPa after 10^5 h creep exposure. Meanwhile, the BC/substrate interface relaxes to a stress of 195 MPa. This result indicates that redistribution of stress in the BC layer takes place during creep exposure.

5. Sensitivity of the Key System Parameters

Based on the results above, it can be seen that thermal gradient and stress will be generated in the TC, BC and substrate layer during steady-state operation, due to the thermal mismatch and different thermal expansion coefficients between the two layers. In the model, thermal and stress distributions are strongly dependent on material parameters and geometrical dimensions of the coated steam dual pipe system. The aim of this section is to analyse effects of these key parameters, which include the TC thickness, TC conductivity, thermal expansion coefficient of the TC, cooling steam temperature and pressure, on the temperature and stress distributions in the dual pipe system using finite element method. Parametric analysis is discussed in detail as follows.

5.1 Coating parameters

5.1.1 Effect of the TC thickness

In the model, the TC layer is used to provide thermal insulation for the primary steam pipe. Here, the difference in temperature across the wall thickness of the TC layer, ΔT, is defined to indicate the thermal insulation of the TC layer. In terms of the heat transfer equation (2), it can be expected that ΔT should increase with the increase of

the coating thickness, d_1, when other parameters in the system remain constant. However, the thickness of the TC layer can only be changed in a given range. If the TC layer is too thick, it will significantly contribute to its accelerated failure [6]. Thus, the variation of ΔT with the thickness of the TC is investigated for a range of h_t values. As exhibited in Fig. 9, it can be seen that the thermal insulation effect of the TC is non-linear with the TC thickness. The d_1 - ΔT curve initially exhibits a highly linear correlation (0.1-0.5 mm), followed by a continuous decrease in slope with increasing the TC thickness. From the current investigation, the thickness of the coating should be reduced as much as possible under the premise of using the TC to provide an effective reduction in the surface temperature of the primary steel pipe.

5.1.2 Effect of the TC thermal conductivity

In addition to the TC thickness, it can be analysed from equation (2) that the thermal conductivity coefficient of the TC is one of the most important factors affecting the thermal insulation of the dual pipe system. Thus, the effect of the TC thermal conductivity, k_1, on the thermal insulation is analysed with d_1 values in the range of 100-3000 μm. Fig. 10 presents the variation of ΔT with the thermal conductivity coefficient of the TC. Obviously, the thermal insulation effect of the TC continuously increases with decreasing the TC thermal conductivity coefficient. In the low thermal conductivity coefficient region, the reduction of the thermal conductivity coefficient can lead to greater thermal insulation. In addition, as the TC thickness increases, the conductivity coefficient of the TC has a greater impact on the thermal insulation. As is well-known, the thermal conductivity coefficient of the TC is strongly dependent on the microstructure of the material and service temperature. Based on this analysis, if the conductivity coefficient of the TC is to be effectively reduced, it is necessary to change the structure of the TC. The effect of microstructural changes on the conductivity coefficient of the TC has been extensively studied in the previous investigations [35-37].

5.1.3 Effect of thermal expansion coefficient of the TC

It is well known that thermal-expansion mismatch stress between the ceramic and metal is one of the most important failure mechanisms in the TBCs system, which hinders the development and use of the TBCs technology [6,33]. Consequently, the effect of thermal expansion coefficient of TC layer on stress distribution is discussed in this

study, as shown in Fig. 11. It can be seen that compared with the hoop stress in the steel pipe, hoop stress in the TC layer changes significantly with increasing the value of thermal expansion coefficient during the steady-state operation. In this condition, the peak hoop stress of TC layer is 592, 379, 166, -46 and -259 MPa when the thermal expansion coefficient takes the values of 6×10^{-6}, 8×10^{-6}, 10×10^{-6}, 12×10^{-6} and 14×10^{-6}/℃, respectively. The comparisons shown in Fig. 11 clearly reveal that the difference in the thermal expansion coefficient between the TC and substrate directly results in a large thermal-expansion mismatch stress at the TC/BC interface, which may ultimately contribute to the spallation failure of the TC layer. Moreover, it is clear that the stress within the TC layer changes from tensile stress to compressive stress with the increase of the thermal expansion coefficient. When the value of thermal expansion coefficient of TC is larger than that of the substrate, the TC is subjected to compressive stress during the steady-state operation. In addition, the variation of the von Mises stress in the TC layer is relatively complicated during the steady-state operation, but it can be seen from Fig. 11(b) that when the thermal expansion coefficient of the TC is greater or less than that of the substrate, the von Mises stress within the TC will increase significantly. From the present investigation, it can be concluded that it may be unrealistic to match the coefficient of thermal expansion between the TC and substrate, so a 3 or 4 layer coating system may be needed in order to further reduce the thermal-expansion mismatch stress of the system.

5.2 Hot and cooling steam parameters

5.2.1 Effect of cooling steam heat transfer coefficient

From equation (4), it can be seen that the effects of heat transfer coefficient of cooling steam and high-temperature steam on the thermal insulation of the dual pipe system are almost the same. In the current investigation, system analysis is carried out by only considering the influence of the cooling steam heat transfer coefficient (h_s) on the thermal insulation as an example. The results for different k_1 values are shown in Fig. 12. As the heat transfer coefficient of the cooling steam increases, the thermal insulation effect of the TC becomes more pronounced, but the thermal insulation effect does not change linearly with the heat transfer coefficient of the cooling steam. It can be seen from Fig. 12 that the change of heat transfer coefficient can greatly affect the

thermal insulation of the TC, when the heat transfer coefficient is very small. Generally, the heat transfer coefficient of the cooling steam is closely related to fluid pressure, geometric shape of heat exchange surface and physical properties of the fluid. In the present model, when h_s=5000 W/(m^2℃), it is obvious from Fig. 12 that the thermal insulation effect of the TC decreases with increasing the TC conductivity. Also, it can be observed from Fig. 12 that the TC does not have the function of thermal insulation during the steady-state operation, if the external counter cooling steam is not provided in the current system. This suggests that the TC can only delay the time of high-temperature attack on the surface of the primary steam pipe. Thus, the coating must work together with the cooling system to achieve the reduction in the surface temperature of the substrate during the steady-state operation.

5.2.2 Effect of cooling steam temperature

In order to investigate the influence of cooling steam temperature, T_o, on the stress distribution in the dual system, a series of FE analyses with T_c=100℃, 200℃, 300℃ and 500℃ are carried out. The results show that radial stress is relatively insignificant in the system. Fig. 13 presents the hoop stress and von Mises stress distributions of the dual pipe system at different outer wall temperatures, where the stress distribution at temperature of 450℃ is also shown as a comparison. By comparing the hoop stress, it can be seen from Fig. 13(a) that the variation of the hoop stress along the wall thickness direction is strongly dependent upon the cooling steam temperature. As the cooling steam temperature decreases continuously, the hoop stress of the system continues to increase. This could be attributed to the temperature difference between the inner and outer walls resulting in the increase of the thermal stress in the dual pipe system. Fig. 13 (b) shows the variation of von Mises stress with cooling steam temperature. The decrease in the cooling temperature greatly increases the von Mises stresses, especially the stress on the TC side. Definitely, it can affect the structural integrity of the system.

5.2.3 Effect of external pressure

The effect of external pressure, P_o, on the stress distribution of the dual pipe system is investigated while other parameters are constant. Four FE analyses with P_c=0 MPa, 10 MPa, 20 MPa, 35 MPa are carried out. The results including hoop stress and von Mises stress along wall thickness direction are shown in Fig. 14, where the stress

distribution curves under an external pressure at 7.5 MPa are also presented as a comparison. Fig. 14 shows that the external pressure can effectively affect the hoop stress distribution although the shape of the hoop stress distribution curve does not change. In the current model, the total hoop stress of the system consists of one part of the hoop stress generated by the temperature load and one part of the hoop stress produced by the pressure load. Due to the same temperature field in the model, hoop stress generated by the temperature load is a constant. However, the complex hoop stress produced by the varying external pressure together with internal pressure will change during the steady-state operation, which contributes to the variation of hoop stress distribution in the system under the different external pressures. Fig. 14(b) reveals the von Mises stress distributions of the system during the steady-state operation. It can be seen that the external pressure can effectively improve the von Mises stress distribution of the TC and primary steam pipe, but can significantly increase the peak von Mises stress of the BC.

6. Discussion

In this study, an innovative steam transfer piping system manufactured from high temperature materials commonly used in current operational power plants is proposed to enable the primary steam pipe in advanced ultra-supercritical power plant to operate at temperature up to 700℃ without the need for nickel-based alloys.

Considering the external (secondary) steam pipe has a relatively uniform through-thickness temperature equal to the exhaust steam temperature, thermal stress in the external pipe is negligible [25]. The structural integrity of the external pipe only under exhaust steam pressure needs to be considered. For the coated primary steam pipe, compared with the mechanical stress generated by the internal pressure and external pressure, thermal stress produced by the thermal gradient along the wall thickness direction is larger during steady-state operation, which plays a significant role in determining the structural integrity of the coated dual pipe system. In the present investigation, an analytical model is built to analyse the thermal stresses of the system. The comparisons shown in Fig. 6(a) clearly reveal that the thermal stress calculated by the analytical model is in agreement with that obtained by the FE model. It proves the validity of the thermal stress analysis model. As mentioned above, a number of contributing factors can affect the temperature and stress fields in the system, and there

is a balance between the thermal insulation capability and thermal stress of the system. Based on this analytical model, an optimization design procedure could be developed to further refine potential design boundaries. Further theoretical studies will be carried out in the future.

As is well-known, for the thermal barrier coatings (typically 8 wt% yttria stabilised zirconia), the BC layer is usually exposed to the high-temperature during steady-state operating conditions which causes BC oxidation and therefore the inevitable formation of the thermally grown oxide (TGO) [6, 17, 19]. The TGO, providing a barrier to oxygen diffusion, grows with the increase of the operation time. In general, the large thermal-expansion mismatch among the TC, TGO and BC can create a significant stress field in the TBCs system [19,38]. With the growth of the TGO during service condition, the stress at the BC and TGO interface can result in interface cracking and observed spallation failure which greatly affect the life of the TBCs system and thereby the primary steam pipe[6]. Thus, TGO is one of the most important factors in examining the reliability of the TBCs system. However, in the present feasibility investigation, more focus has been made on the fundamental thermal and stress analyses of the coated dual pipe system, instead of the formation of the TGO.

The results obtained by the FE illustrate that the TC layer withstands the most extreme steam temperature, and contributes to the effective reduction in the surface temperature of the steel pipe, as shown in Fig. 5. However, due to the counter-cooling design, high thermal stress is generated by temperature gradient between the wall thicknesses. The greater temperature differences, the higher thermal stresses in the system are produced. Since hoop stress is much larger than the radial stress during the steady-state operation, it implies that hoop stress plays a major role in determining the structural integrity of the system [27]. Additionally, the sum of mechanical stress induced by the internal and external loads and thermal-expansion mismatch stresses in the system generated by the significant difference in thermo-mechanical properties of the different layers are less than the yield strength of the ceramic and metal material. Consequently, from the current temperature and stress fields as well as creep analyses results of the system, it may be feasible to design such a novel engineering steam pipeline, although a number of further technical challenges, i.e. the optimal thermal design, the most appropriate methods of manufacturing, assessing the structural integrity of counter-flow cooled component, the lifetime of the system, are necessary to

be addressed, and a combined theoretical, experimental and numerical investigation is inevitably required. Creep relaxation behaviour of the proposed TBC system, especially the stress evolution in the BC layer, is also observed in this work, as shown in Fig. 7. During the long-term creep exposure, creep deformation of the BC layer greatly influences the stress redistribution in the TBC system, and results in the continuous reduction of the stress in the BC layer with the creep time. This results are consistent with Busso and Fan's investigations [16,19]. Compared with the extensive stress relaxation of the BC layer, creep does not play a significant role in the stress distribution of the TC and substrate, and only greatly reduces the stress level at the TC/BC interface and BC/substrate interface. This phenomenon may be attributed to the limited creep strain in the TC and substrate layer. It can be seen from theoretical equation (16) that the creep stain rate of the TC during long-term creep exposure is much lower than that of the BC layer at the service temperature and stress levels, and thereby the stress distributions in the TC layer are not affected. For the substrate layer, since the TC layer and external counter-cooling steam effectively reduce the temperature of the inner and outer surfaces of the steel pipe seen from the temperature profile in Fig. 5, in addition to the BC/substrate interface subjected to the temperature of 560℃, most of the steel pipes are exposed to the temperature below 560℃. Owing to the good creep resistance of P91 steel, a large amount of creep strains cannot be observed in the substrate.

The effect of several key factors on the temperature and stress distributions is also analysed in the present investigation. It can be seen from Figs. (9), (10) and (12) that the TC thickness, conductivity coefficient of TC layer and heat transfer coefficient of cooling steam have a significant impact on temperature field, and thereby influence the stress field of the coated dual pipe system. In addition, the thermal expansion coefficient of the TC, cooling steam temperature and the external pressure greatly affect the stress distribution of the system. It is clear from Fig. (14) that the external cooling steam pressure can effectively improve the stress distribution of the primary steam pipe. In the current system, these factors work together to influence the temperature and stress distributions of the system.

7. Conclusions

(1) An analytical model is developed which is capable to calculate the temperature profiles and thermal stress fields of the coated steam dual pipe system during steady

state operation.

(2) Due to the significant difference in the thermal and mechanical properties of the coating and substrate pipe, thermal stresses generated due to the thermal gradient through the pipe wall are larger than the mechanical stresses generated by the combined effects of the internal steam pressure in the primary steam pipe and external pressure from the counter-flow cooling steam.

(3) Hoop stress is much larger than the radial stress during the steady-state operation, which plays a major role in determining the structural integrity of the system.

(4) Compared with the stress relaxation of the coating and substrate pipe, creep has a significant impact on the stress distribution within the coating layer.

(5) Several key governing parameters have been identified, such as the coating thickness, conductivity, thermal expansion, heat transfer coefficient of cooling steam, cooling steam temperature and cooling steam pressure, are found to have a significant effect on thermal and stress distributions during steady-state operation. Among these investigated parameters, the coating thickness may be the most sensitive factors since the increase of coating thickness directly contributes to the increase of temperature gradient along the wall thickness direction, and therefore results in the increase of thermal stress in the dual pipe system.

A number of research challenges discussed in the current study are required to be addressed to enable the feasibility of the dual pipe concept in the future work. More realistic material combinations and properties and the dimensions of the coating-pipe system used in this study need to be carefully considered in order to optimize the system's performance. For a more detailed system analysis to be carried out in the future, a classical anisothermal viscoplastic model can be employed to study the dual pipe system [40]. More detailed numerical analyses should be carried out to evaluate the effect of the thermal gradients and the stresses generated during start-ups / shut downs or possible shakedown operations. Several time- and cycle-dependent phenomena, such as the formation of TGO, the interdiffusion of the high concentration elements between the different interfaces as well as premature spallation failure during the steady-state operation, should be further investigated. One of the main challenges is how to access the structural integrity of the proposed components under thermo-mechanical loadings. Therefore, nonlinear damage mechanics models will be developed to model creep and

combined creep-fatigue behaviour. These potential problems should be considered in the future work.

Acknowledgements

This work is supported by the Engineering and Physical Sciences Research Council (EPSRC) through the project "Novel High Temperature Steam Transfer Pipes" [Grant number: EP-R000859-1] and the National Natural Science Foundation of China (51805274). The authors would also like to thank EDF UK for technical support.

References

[1] F. Abe, Progress in creep-resistant steels for high efficiency coal-fired power plants, J. Press. Vess-t. Asme 138(4) (2016) 1-21.

[2] N. Saito, N. Komai, K. Hashimoto, Evaluation of stress relaxation cracking susceptibility in Alloy 617 for advanced USC boilers, Int. J. Pres. Ves. Pip. 168 (2018) 183-190.

[3] M. Speicher, F. Kauffmann, J.H. Shim, M. Chandran, Microstructure evolution in alloy 617 B after a long-term creep and thermal aging at 700 °C, Mater. Sci. Eng. A-struct 711 (2018) 165-174.

[4] Z.H. Zhong, Y.F. Gu, Y. Yuan, Z. Shi, A new wrought Ni–Fe-base superalloy for advanced ultra-supercritical power plant applications beyond 700 °C, Mater. Lett. 109 (2013) 38-41.

[5]H.I. Khan, N.Q. Zhang, W.Q. Xu, Z.L. Zhu, D.F. Jiang, H. Xu, Effect of maximum stress intensity factor, loading mode, and temperature on corrosion fatigue cracking behavior of Inconel 617 in supercritical water, Int. J. Fatigue 118 (2019) 22-34.

[6] N.P. Padture, M. Gell, E.H. Jordan, Thermal barrier coatings for gas-turbine engine applications, Science 296 (2002) 280-284.

[7] G. Boissonnet, C. Boulesteix, G. Bonnet, J. Balmain, F. Pedraza, Thermal transport properties of new coatings on steels for supercritical steam power plants, Oxid. Met. 88 (2017) 191–202.

[8] A.G. Evans, D.R. Mumm, J.W. Hutchinson, G.H. Meier, F.S. Pettit, Mechanisms controlling the durability of thermal barrier coatings, Prog. Mater. Sci. 46 (2001) 505-553.

[9] P. Skalka, K. Slámečka, J. Pokluda, L. Čelko, Finite element simulation of stresses in a plasma-sprayed thermal barrier coating with a crack at the TGO/bond-coat interface, Surf. Coat. Technol. 337 (2018) 321–334.
[10] A. G. Koushali, M. Sameezadeh, M. Vaseghi, P. Safarpour, Analytical and numerical investigations of the crack behavior in thermal barrier coatings under the trip thermal load, Surf. Coat. Technol. 337 (2018) 90–96.
[11] E.P. Busso, Z.Q. Qian, M.P. Taylor, H.E. Evans, The influence of bondcoat and topcoat mechanical properties on stress development in thermal barrier coating systems, Acta Mater. 57 (2009) 2349–2361.
[12] A.M. Limarga, R. Vaßen, D.R. Clarke, Stress distributions in plasma-sprayed thermal barrier coatings under thermal cycling in a temperature gradient, J. Appl. Mech-t. Asme. 78 (2011) 1-9.
[13] M.P. Taylor, H.E. Evans, E.P. Busso, Z.Q. Qian, Creep properties of a Pt–aluminide coating, Acta Mater. 54 (2006) 3241–3252.
[14] M.P. Taylor, H.E. Evans, C.B. Ponton, J.R. Nicholls, A method for evaluating the creep properties of overlay coatings, Surf. Coat. Technol. 124 (2000) 13–18.
[15] D. Pan, M.W. Chen, P.K. Wright, K.J. Hemker, Evolution of a diffusion aluminide bond coat for thermal barrier coatings during thermal cycling, Acta Mater. 51 (2003) 2205–2217.
[16] E.P. Busso, J. Lin, S. Sakurai, M. Nakayama, A mechanistic study of oxidation-induced deformation in a plasma-sprayed thermal barrier coating system. Part I: model formulation, Acta mater. 49 (2001) 1515–1528.
[17] W.J. Brindley, J.D. Whittenberger, Stress relaxation of low pressure plasma-sprayed NiCrA1Y alloys, Mater. Sci. Eng. A-struct 163 (1993) 33-41.
[18] J.S. Jiang, W.Z. Wang, X.F. Zhao, Y.Z. Liu, Z.M. Cao, P. Xiao, Numerical analyses of the residual stress and top coat cracking behavior in thermal barrier coatings under cyclic thermal loading, Eng. Fract. Mech. 196 (2018) 191-205.
[19] B. Li, X.L. Fan, K. Zhou, T.J. Wang, A semi-analytical model for predicting stress evolution in multilayer coating systems during thermal cycling, Int. J. Mech. Sci. 135 (2018) 31–42.
[20] M.Bäker, Influence of material models on the stress state in thermal barrier coating simulations, Surf. Coat. Technol. 240 (2014) 301–310.

[21] R.A. Miller, C.E. Lowell, Failure mechanisms of thermal barrier coatings exposed to elevated temperatures, Thin Solid Films 95 (1982) 265-273.

[22] R. Ghasemi, R. Shoja-Razavi, R. Mozafarinia, H. Jamali, Comparison of microstructure and mechanical properties of plasma-sprayed nanostructured and conventional yttria stabilized zirconia thermal barrier coatings, Ceram. Int. 39(8) (2013) 8805–8813.

[23] X.Q. Cao, R. Vassen, D. Stoever, Ceramic materials for thermal barrier coatings, J. Eur. Ceram. Soc. 24(1) (2014) 1–10.

[24] B. Li, Y. Li, J. Su, A combined interface element to simulate interfacial fracture of laminated shell structures, Compos. Part. B-eng 58 (2014) 217–227.

[25] C. Wales, M. Tierney, M. Pavier, P. Flewitt, Reducing steam transport pipe temperatures in power plants, Energy, 2019. (Under review)

[26] D. J. Johns, Thermal Stress Analyses, 1st Ed., Pergamon, 1965.

[27] Vallourec & Mannesmann Tubes. T/P91 tubing handbook[R]. Boulogne France: Vallourec & Mannesmann Tubes, 2012.

[28] H. Dong, G.J. Yang, H.N. Cai, H. Ding, C.X. Li, C.J. Li, The influence of temperature gradient across YSZ on thermal cyclic lifetime of plasma-sprayed thermal barrier coatings, Ceram. Int. 41 (9) (2015) 11046–11056.

[29] S. Gadag, G. Subbarayan, W. Barker, Thermo-elastic properties of dense YSZ and porous Ni–ZrO_2 monolithic and isotropic materials, J. Mater. Sci. 41 (4) (2006) 1221–1232.

[30] A335 P91 – Special alloy steel for high temperature application in power plants. https://www.multimetalsindia.com/blog/astm-a335-p91material/#p91_material_properties, 2019 (accessed 23 January 2003).

[31] H. A. E. Hawa, A. Bhattacharyya, D. Maurice, Modeling of thermal and lattice misfit stresses within a thermal barrier coating, Mech. Mater. 122 (2018) 159–170.

[32] M. Ahrens, S. Lampenscherf, R. Vassen, D. Stover, Sintering and creep processes in plasma-sprayed TBCs, J. Therm. Spray Technol. 13 (2004) 432–442.

[33] P. Bednarz, Finite element simulation of stress evolution in thermal barrier coating systems, Ph.D. thesis, Forschungszentrum Julich GmbH, Julich,2006.

[34] R. Lim, Numerical and experimental study of creep of Grade 91 steel at high temperature, Ph.D. thesis, École Nationale Supérieure des Mines de Paris, 2011.

[35] M. Khan, Y. Zeng, N.N. Hua, Z.H. Lan, Y.Z. Wang, Optimizing the structure and properties of Y_2O_3 stabilized zirconia: An atmospheric plasma spray (APS) and solution precursor plasma spray (SPPS) based comparative study, Ceram. Int. 44 (2018) 18135-18142.

[36] S.R. Gul, M. Khan, Y. Zeng, B. Wu, Understanding the improved stability and reduced thermal conductivity of yttria stabilized zirconia: A combined experimental and atomistic modeling study, Comp. Mater. Sci. 153 (2018) 208-216.

[37] H.Q. Lavasani, Z.V.N. Ehsani, S.T. Masoule, Comparison of the effect of sintering on the microstructure, micro hardness and phase composition of conventional and nanostructured YSZ TBCs, Ceram. Int. 43 (2017) 12497-12504.

[38] Z. Chen, H.M. Huang, K. Zhao, W.B. Jia, L. Fang, Influence of inhomogeneous thermally grown oxide thickness on residual stress distribution in thermal barrier coating system, Ceram. Int. 44 (2018) 16937–16946.

[39] W. C. Jiang, Y. Luo, B.Y. Wang, S.T. Tu, J.M. Gong, Residual stress reduction in the penetration nozzle weld joint by overlay welding, Mater. Design 60 (2014) 443–450.

[40] A. Benaarbia, J.P. Rouse, W. Sun, A thermodynamically-based viscoelastic-viscoplastic model for the high temperature cyclic behaviour of 9–12% Cr steels, International Journal of Plasticity 107 (2018) 100–121.

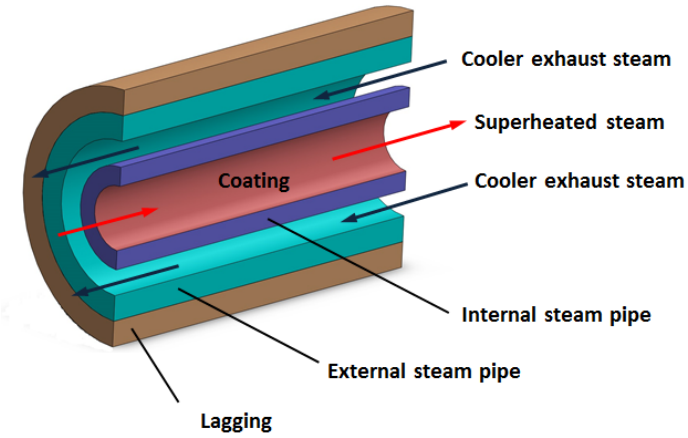

Fig. 1 Schematic diagram of the coated steam dual pipe system for use in advanced ultra-supercritical power plant. The internal (primary) steam pipe conveys steam from the boiler outlet to the high pressure steam turbine, with an external (secondary) steam pipe conveying the counter-cooling steam

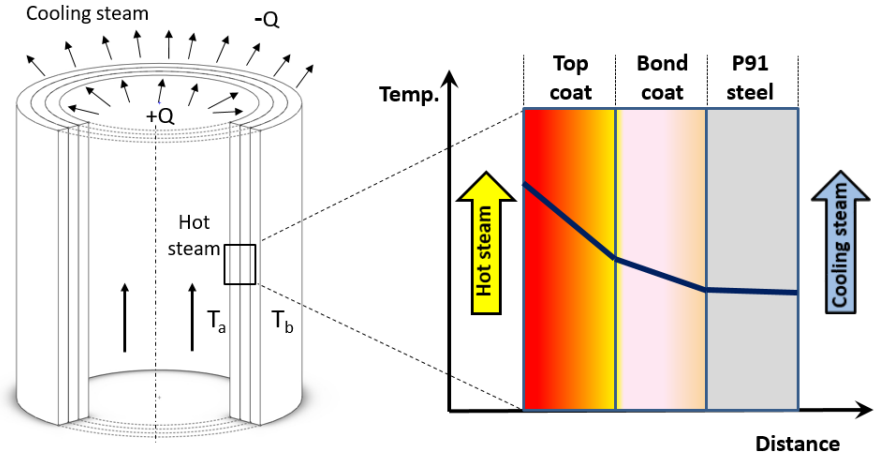

Fig. 2 Sectional schematic diagram of the coating-pipe structure, with a schematic of the steady-state temperature distribution through the TBC and primary steam pipe

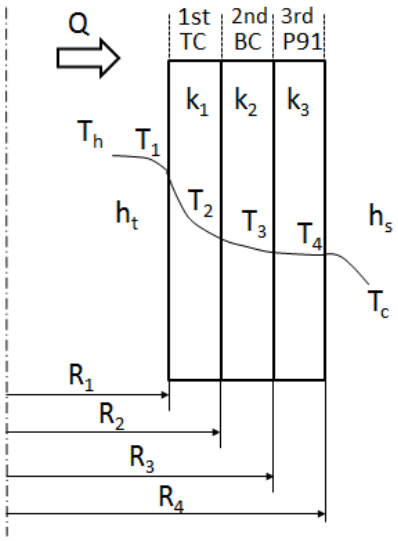

Fig. 3 Axisymmetric model of heat transfer during steady-state operation

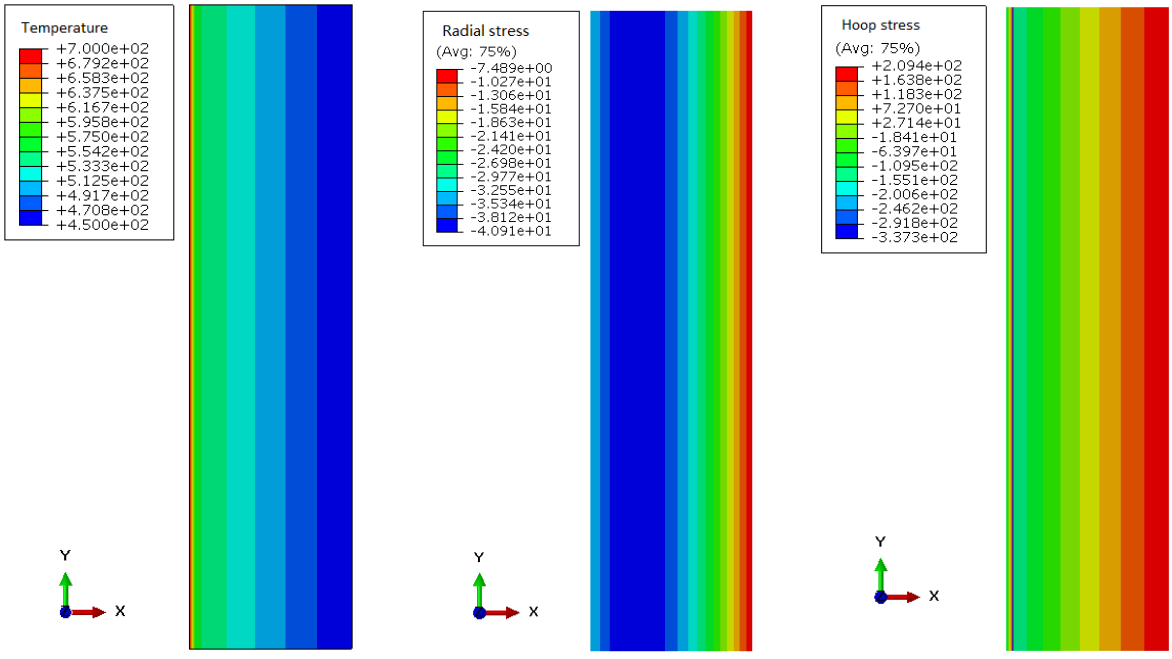

(a) (b) (c)

Fig. 4 Temperature and stress distribution contour plots of the coated primary steam pipe during the steady-state operation: (a) temperature; (b) radial stress; (c) hoop stress

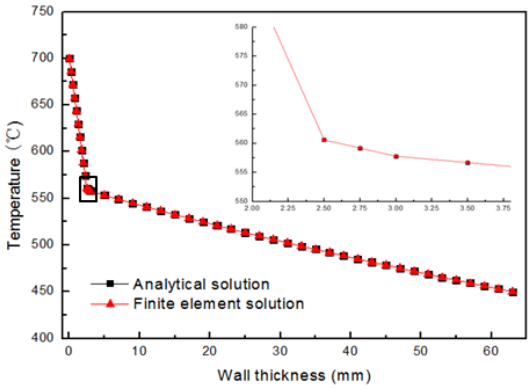

Fig. 5 Comparisons of temperature field in the coated primary steam pipe calculated by the analytical solution and finite element (FE)

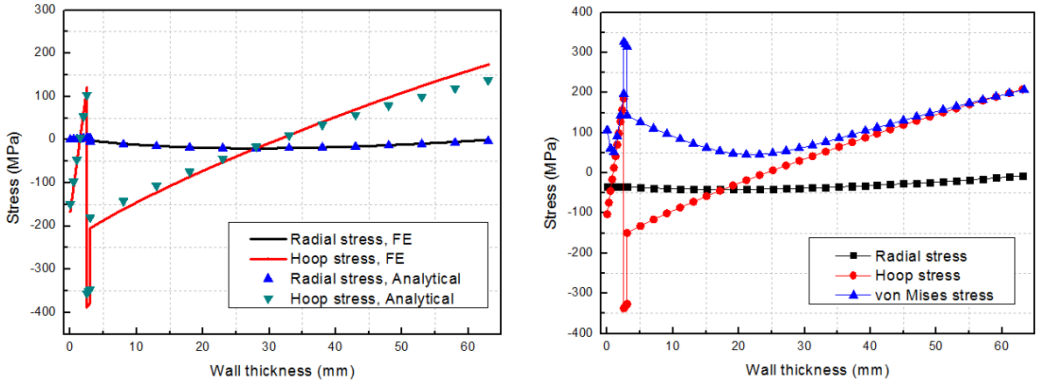

(a) (b)

Fig. 6 Stress distribution in the coat-primary steam pipe system: (a) thermal stress calculated by the analytical solution and finite element (FE); (b) the stress including thermal and mechanical stress calculated by FE

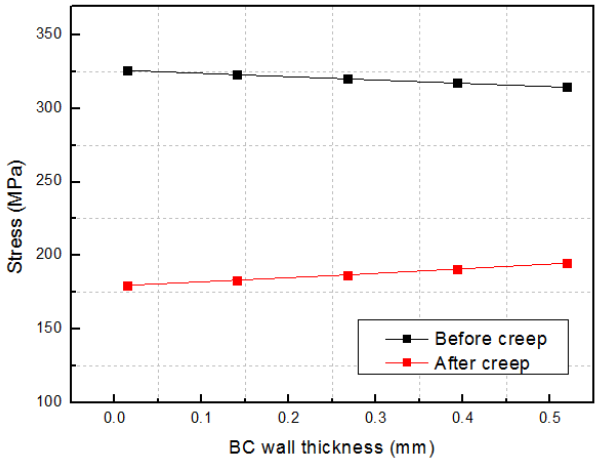

Fig. 7 The variation of stress along BC wall thickness before and after creep

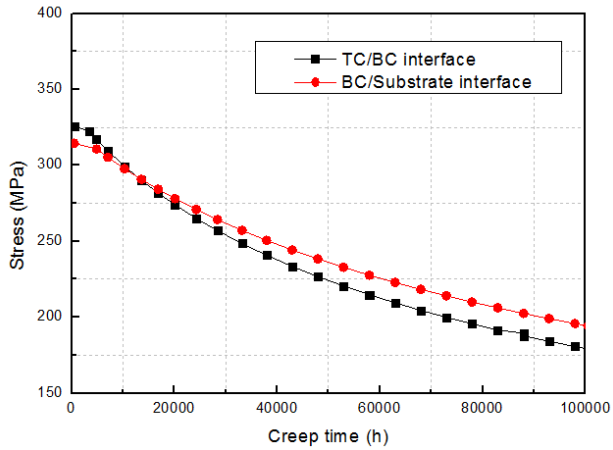

Fig. 8 Stress relaxation at the TC/BC interface and BC/substrate interface during long-term creep exposure

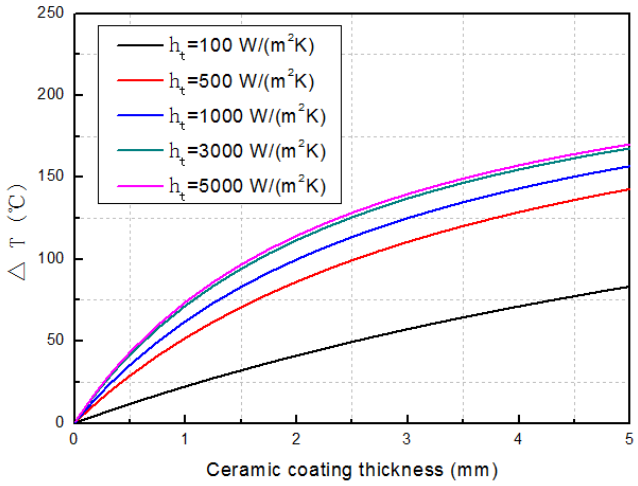

Fig. 9 Effect of the TC thickness on the thermal insulation of the TC during steady-state operation

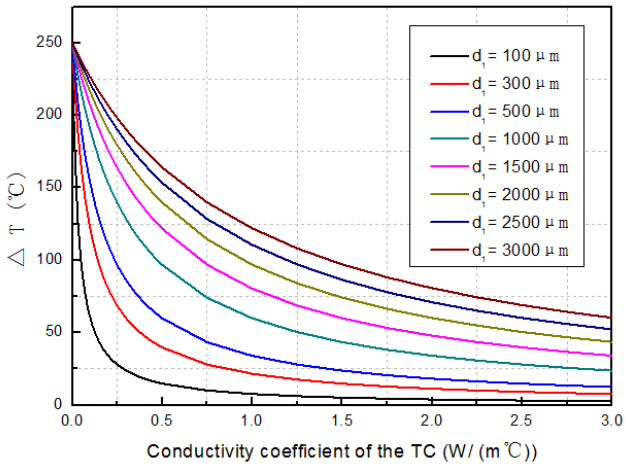

Fig. 10 Effect of conductivity coefficient on the thermal insulation of the TC during steady-state operation

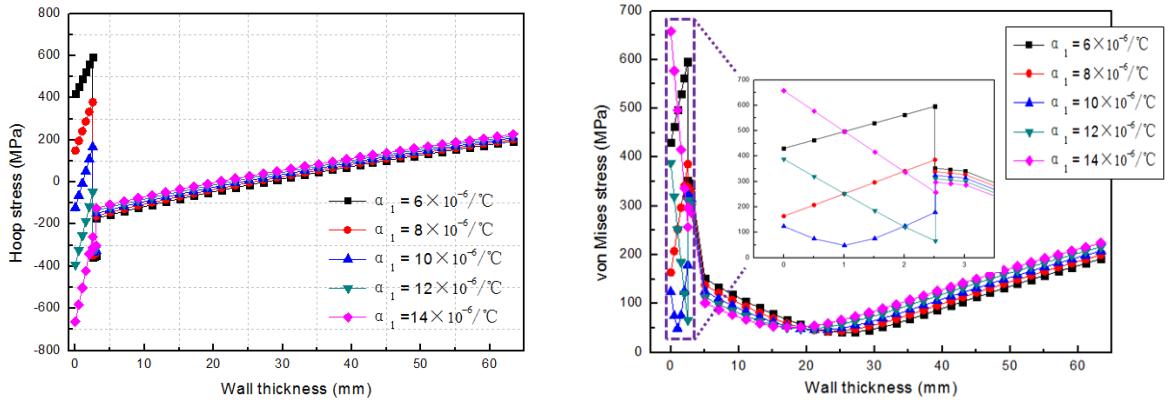

Fig. 11 Effect of thermal expansion coefficient of the TC on stress distribution during steady-state operation: (a) hoop stress; (b) von Mises stress

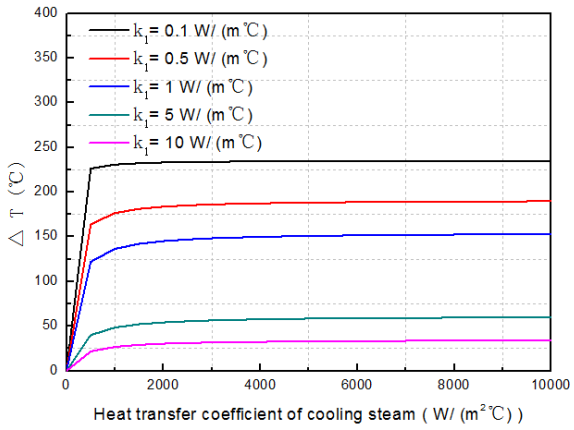

Fig. 12 Effect of heat transfer coefficient of cooling steam on the thermal insulation of the TC during steady-state operation

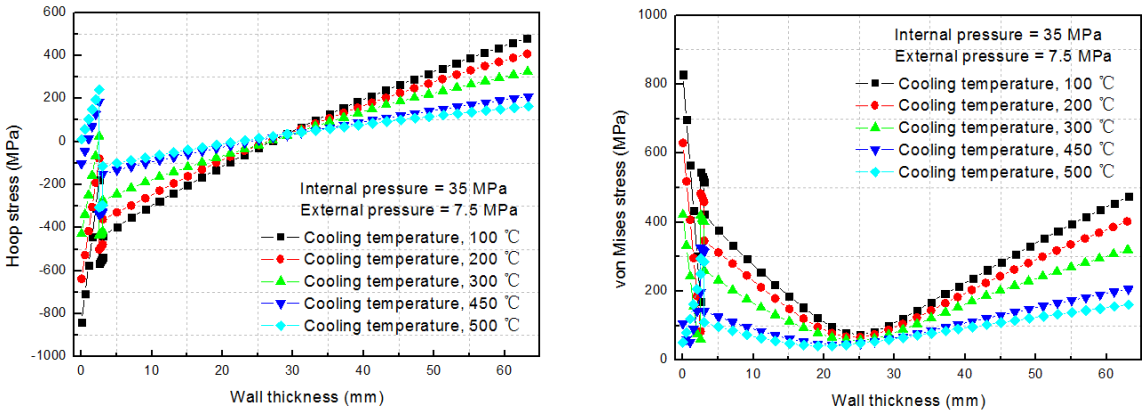

(a) (b)

Fig. 13 Stress distribution of the coated primary steam pipe at different outer wall temperatures: (a) hoop stress; (b) von Mises stress

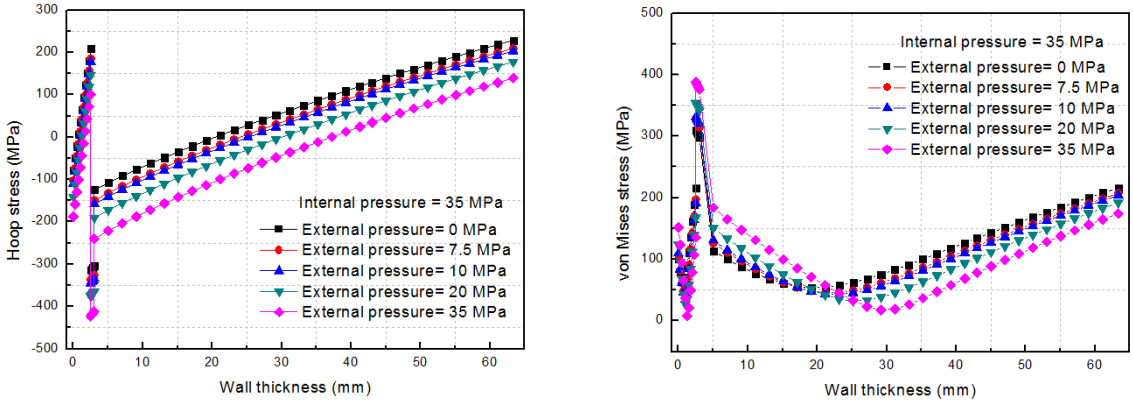

(a) (b)

Fig. 14 Stress distribution of the coated primary steam pipe system under the different external pressures: (a) hoop stress; (b) von Mises stress

Table 1 The key geometries of the coated dual pipe system and the assumed steady state steam conditions

	Material	Temperature (℃)	Pressure (MPa)	Inner diameter (mm)	Thickness (mm)
TC	YSZ	700	35	234	2.5
BC	NiCoCrAlY			239	0.5
Primary pipe	P91			240	60
Secondary pipe	T23	450	7.5	450	20

Table 2 Temperature dependent material properties of the top coat (TC), bond coat (BC) and the internal steam pipe for a range of temperatures [27-31]

Material	T (℃)	E (GPa)	ν	Yield strength (MPa)	Density (kg/m^3)	CTE (10^{-6}/℃)	Conductivity (W/m℃)	Specific heat (J/(kg℃))
P91	20	218	0.3	488	7770		26	440
	100	213		461		10.9	27	480
	200	207		441		11.3	28	510
	300	199		427		11.7	28	550
	400	190		396		12.1	29	630
	450	186				12.1	29	630
	500	181		360		12.3	30	660
	550	175		331		12.4	30	710
	600	168		285		12.6	30	770
	650	162		206		12.7	30	860
8YSZ	20	204	0.10		6037	9.68	1.2	500
	800	179	0.11			9.88		
NiCoCrAlY	20	200	0.30	868	7711	12.5	5.8	628
	800	145	0.32	191		14.3	14.5	

Table 3 Creep properties of the TC, BC and P91 [11, 12, 32-34]

Material	B($MPa^{-n}h^{-1}$)	n	T (℃)
TC	7.71×10^{-27}	4	550
	1.42×10^{-24}	4	600
	1.53×10^{-22}	4	650
	1.01×10^{-20}	4	700
BC	6.62×10^{-17}	3	550
	4.35×10^{-15}	3	600
P91	1.56×10^{-55}	20.35	500
	6.97×10^{-45}	16.76	550
	8.42×10^{-27}	9.94	600